RESEARCH ARTICLE

3D Printing of Layered Gradient Pore Structure of Brain-like Tissue

Na Pei[1,2], Zhiyan Hao[1,2], Sen Wang[1,2], Binglei Pan[1,2], Ao Fang[1,2], Jianfeng Kang[3], Dichen Li[1,2], Jiankang He[1,2], Ling Wang[1,2]*

[1]State Key Laboratory for Manufacturing System Engineering, Xi'an Jiaotong University, 710054, Xi'an, Shaanxi, China
[2]School of Mechanical Engineering, Xi'an Jiaotong University, 710054, Xi'an, ShanXi, China
[3]Jihua Laboratory, Foshan, 528000, Guangdong, China

Abstract: The pathological research and drug development of brain diseases require appropriate brain models. Given the complex, layered structure of the cerebral cortex, as well as the constraints on the medical ethics and the inaccuracy of animal models, it is necessary to construct a brain-like model *in vitro*. In this study, we designed and built integrated three-dimensional (3D) printing equipment for cell printing/culture, which can guarantee cell viability in the printing process and provide the equipment foundation for manufacturing the layered structures with gradient distribution of pore size. Based on this printing equipment, to achieve the purpose of printing the layered structures with multiple materials, we conducted research on the performance of bio-inks with different compositions and optimized the printing process. By extruding and stacking materials, we can print the layered structure with the uniform distribution of cells and the gradient distribution of pore sizes. Finally, we can accurately print a structure with 30 layers. The line width (resolution) of the printed monolayer structure was about 478 μm, the forming accuracy can reach 97.24%, and the viability of cells in the printed structure is as high as 94.5%.

Keywords: Brain-like model; Layered gradient structure; Integrated cell printing/culture equipment; 3D bio-printing

*Correspondence to: Ling Wang, State Key Laboratory for Manufacturing Systems Engineering, Xi'an Jiaotong University, Xi'an 710054, Shaanxi, China; menlwang@mail.xjtu.edu.cn

Received: March 22, 2021; **Accepted:** April 20, 2021; **Published Online:** June 15, 2021

(This article belongs to the *Special Section: Bioprinting of 3D Functional Tissue Constructs*)

Citation: Pei N, Hao Z, Wang S, *et al*., 2021, 3D Printing of Layered Gradient Pore Structure of Brain-like Tissue. *Int J Bioprint*, 7(3):359. http://doi.org/10.18063/ijb.v7i3.359

1. Introduction

According to the statistics from the World Health Organization, the burden of brain diseases throughout the world has exceeded that of cardiovascular diseases and cancer, accounting for 28%[1]. At present, the models used for brain pathology research and new drug development are mainly derived from animal models[2], which not only have long cycles but also display huge differences as compared to the human brain tissue[3], leading to a failure rate of drug development as high as 95%. In addition, the two-dimensional (2D) cell model is the main approach for pathological research, but due to lacking the interactions of cell-cell and cell-extracellular matrix (ECM), the neurons cultured on 2D cell culture dishes show significant deficiency[4-6]. Compared with the traditional tissue engineering methods, 3D bioprinting technology can be used to manufacture biomimetic tissue with complex structure through a highly automated manufacturing platform. Three-dimensional (3D) bioprinting technology has high precision and repeatability, which has great potential in achieving the envisioned goal of tissue-specific composition and localization of simulated cells and extracellular components[7]. The 3D bioprinting processes can be classified into five main categories: (i) Extrusion bioprinting[8,9], (ii) stereolithography bioprinting[10], (iii) inkjet bioprinting[11], (iv) laser-assisted bioprinting[12], and (v) microvalve-based bioprinting[13]. Extrusion-based bioprinting technology is the most commonly used bioprinting method because of its fast printing speed and a wide variety of bio-inks that can be printed.

Native tissues and/or organs possess complex hierarchical porous structures that confer highly-specific cellular functions[14]. The highly complex hierarchical porous structures are commonly found in most biological tissues such as skin[15-17], corneal[18], and even bone[19]. The importance of such hierarchical porous structures in native tissues has been critically reviewed elsewhere[20,21]. At present, 3D tissue engineering has been used to print the hierarchical porous structures in skin, blood vessels, esophagus, bladder, cartilage[22-28], and other tissues. Ng *et al*.[17] used a two-step drop-on-demand bioprinting strategy to manipulate the microenvironment to fabricate 3D biomimetic hierarchical porous collagen-based structures found in native skin tissue. The differences between the two manufacturing methods (3D bioprinting and manual-casting) are also compared. The results show that the two-step bioprinting strategy enables the homogeneous distribution of printed cells in a highly controlled manner as compared to the manual casting approach. However, there is a transition region between layers in the layered structure obtained by the 3D bioprinting method, while the aperture size in the transition region is uncontrollable. Nam *et al*.[29] used the dragging technique based on 3D extrusion method to manufacture the multi-layered hierarchical structure of the esophagus, it allowed the production of tubular structures with an adjustable line width and pore size. Moreover, their study also proved that porous structure can provide a more favorable environment for cell proliferation. However, the stretching properties vary depending on the viscosity of the material, and there are differences and limitations in pore size control for each self-supporting material. Sun *et al*.[30] incorporated biochemical stimulus with different growth factor releasing and biomechanical stimulus with small pore sizes to induce better chondrogenesis to create the dual-factor releasing and gradient-structured cartilage construct. The results indicated that the gradient scaffold group showed better chondroprotective effects with a significantly higher histological grading compared with the nongradient groups over the 24 weeks *in vivo*. However, the change of the pore size in this study was obtained by changing the spacing between the printed lines, which did not change the pore size in the printed structures.

Xu *et al*.[31] utilized a single type of hydrogel by changing the weight/volume ratio of Gelatin-methacryloyl (GelMA) to bioprint the bilayer tubular construct which has smaller pores in the inner layers (6% GelMA) and larger pores in the outer layers (4% GelMA). The results also indicated that the difference in pore sizes may have helped prevent each of these cell types from crossing their respective layers. Although the cells had a high survival rate after printing, the 3-(4,5-dimethylthiazol-2-yl)-2,5-diphenyltetrazolium bromide results showed that the cells in the printed structure almost did not proliferate after the 7 days of culture, which may be related to the printing inks in this research did not have the ability to make the cells growth rapidly. However, because of the complex composition and complicated structure of the brain tissue, it is rarely used in the brain.

The cerebral cortex is a layered gray matter covering the surface of the cerebral hemisphere. The lamellar structure is one of the most obvious characteristics of the cerebral cortex[32]. It has a typical structure with six layers and each has specific neurons. The six-layer structure is composed of the molecular layer (layer I), the external granule cell layer (layer II), the external pyramidal cell layer (layer III), the internal granule cell layer (layer IV), the internal pyramidal cell layer (layer V), and the multiform layer (layer VI). The thickness of the cortex in different functional areas ranges from 2 mm to 5.2 mm, and the thickness of each layer ranges from 200 μm to 1000 μm. The researchers believe that the gradient distribution of ECM or the soluble signal factors is likely to be the inducement of the directional growth and migration of neurons. They also studied the effects of gradient distribution of matrix hardness[33] and growth factors[34] on the directional growth of neurons. Various characteristic parameters of the natural cerebral cortex are the important basis to determine the target parameters of the brain-like cortex model with a layered gradient structure which we constructed in this study. Brain tissue has obvious biophysical characteristics, with the modulus of much lower than that of the heart, cartilage, etc. (the modulus of newborn brain tissue is about 110 Pa, and that of an adult brain tissue is about 500 – 1000 Pa)[35]. The porosity of the cerebral matrix has a greater influence on cell migration and metabolism[36-41]. Designing and manufacturing the brain-like model with similar pore size to natural tissues are more conducive to cell migration and nutrient exchange. Therefore, the manufacturing targets of the layered gradient structure that imitates the cerebral cortex are: (i) The bio-inks containing components with different concentration, (ii) the modulus of the printed structure which is as close as possible to 1000 Pa, and (iii) the appropriate internal pore size (30 – 150 μm) of the printed structure.

In this study, we have designed and built a set of integrated equipment for cell printing/culture, which can realize the target of printing a structure with multiple cells and multiple materials. This equipment can provide a suitable environment during the printing process for the cells to survive. Furthermore, this equipment also provides a long-term cultivation environment for the printed structure, which can solve the problem of separating the printed structure from the printing process to culture process in the traditional 3D printing method and can reduce the risk of cell contamination during the process

of transferring the printed structure to an incubator after printing. Moreover, we also optimize the printing process by adjusting the printing parameters of the bio-inks and the pre-processing and post-processing conditions of the bio-inks so that we can accurately control the compression modulus of the printed structure. Collagen is the main component of natural ECM, accounting for about 30% of the total protein of human body[14], which provides structural stability and strength to numerous tissues such as skin, bone, cartilage, or even teeth. Therefore, in this study, collagen was added to the bio-inks to increase the survival rate of the cells in printed structure. Then, the distribution of pore size in brain tissue was simulated by changing the concentration of collagen in bio-inks to alter the inner pore size of printing structure. Therefore, an artificial brain-like tissue model with a gradient distribution of pore size was constructed *in vitro*.

2. Materials and methods

2.1. Building an integrated cell printing/culture equipment

The integrated cell printing/culture equipment consists of both hardware and software. The hardware consists of three parts: Mobile control module, material extrusion module, and environment control module. The main components of the mobile control module and the material extrusion module were placed outside of the environment control module to avoid the corrosion of the precision components caused by humidity and other conditions in the printing environment. The software was based on the VC language which can realize the coordinated control of the mobile platform and the material extrusion module. QT5.8 programming software was used to write a set of graphical control software. We can achieve the goal of printing a brain-like layered structure with multiple bio-inks and multiple cells using multi-nozzles. Finally, the printed tissue can be cultured in the equipment after the printing process. Moreover, the environment within the equipment can be controlled to provide a suitable environment for the survival of cells, formation of bio-inks, and the culture of printed tissue. The integrated cell printing/culture equipment is shown in **Figure 1**, and the parameters of each part of this equipment are shown in **Table 1.**

2.2. Printing principle

Multiple nozzles were used to print the layered gradient brain-like structure by the extrusion method. Each nozzle contained a bio-ink with different compositions and different cells (**Figure 2B**), and all the nozzles printed the structure layer by layer in turn until the printing process was completed.

Table 1. Parameters of the integrated cell printing/culture equipment

Environment control module	Temperature		0 – 50±0.8°C
	Humidity		50 – 95%
	Oxygen concentration		0 – 5%
Material extrusion module	Channels		4
	Maximum stroke		90 mm
	Linear velocity range		7.49 μm/min – 79.4 mm/min
	Stroke resolution		0.165 μm
Motion control module	Stroke	X	150 mm
		Y	150 mm
		Z	150 mm
	Speed	X,Y	0 – 50 mm/s
	Reposition accuracy	X,Y,Z	10 μm
	Position Accuracy	X,Y,Z	20 μm

2.3. Preparation of the bio-inks

The bio-inks used for 3D cell printing needed to be both printable and biocompatible. Under certain conditions, gelatin and sodium alginate had higher viscosities which were easy to form and had good printing properties, but they were poorly biocompatible. Collagen and silk fibroin had good biocompatibility, but they were difficult to form and cannot print. Therefore, it was difficult to use a single biomaterial to meet the requirements of the printing. In this paper, gelatin and sodium alginate were mixed as the basic components of the bio-ink, and collagen was added as a regulating factor to form the final bio-ink, which has been proven to have good biocompatibility and printability.

The sodium alginate (medium viscosity, purity ≥98%) and gelatin (from pigskin, medium-strength) used in this experiment were purchased from Sigma company. Collagen was collagen type I, which was extracted from rat tail by our research group, and its concentration was 6 mg/ml. According to the preliminary experiment, we selected 6 wt% gelatin and 1 wt% sodium alginate as the basic bio-inks, and the collagen with different concentrations was added as the regulatory factor. By changing the concentration of collagen in the bio-ink (the concentrations of collagen are 1.5 mg/ml, 1 mg/ml, and 0.5 mg/ml, which are denoted as G6A1C1.5, G6A1C1, and G6A1C0.5, respectively), we could obtain the bio-inks that can print the layered gradient brain-like structure.

According to the characteristics of collagen that gelates at high temperature and of gelatin at low temperature, we developed a configuration process to mix the bio-inks (**Figure 3**).

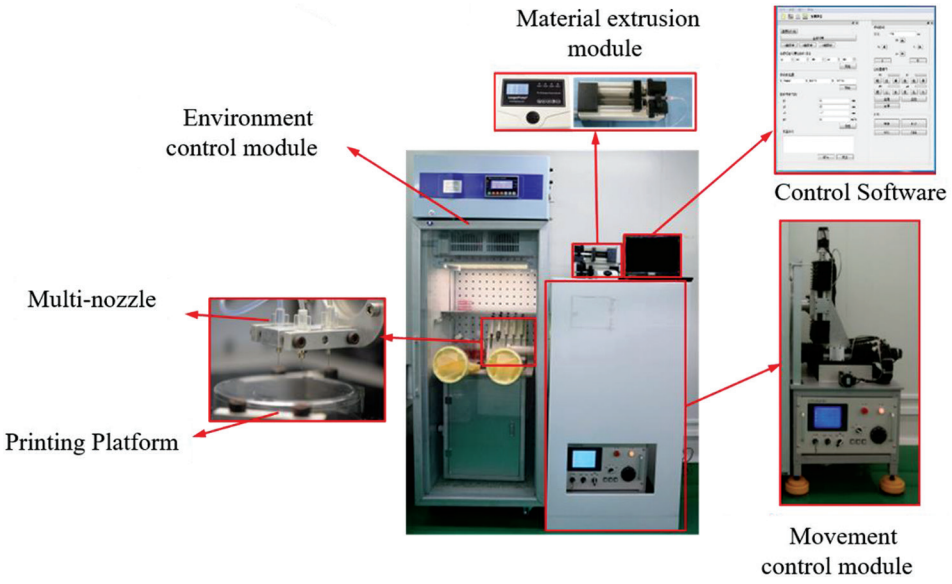

Figure 1. The integrated cell printing/culture equipment.

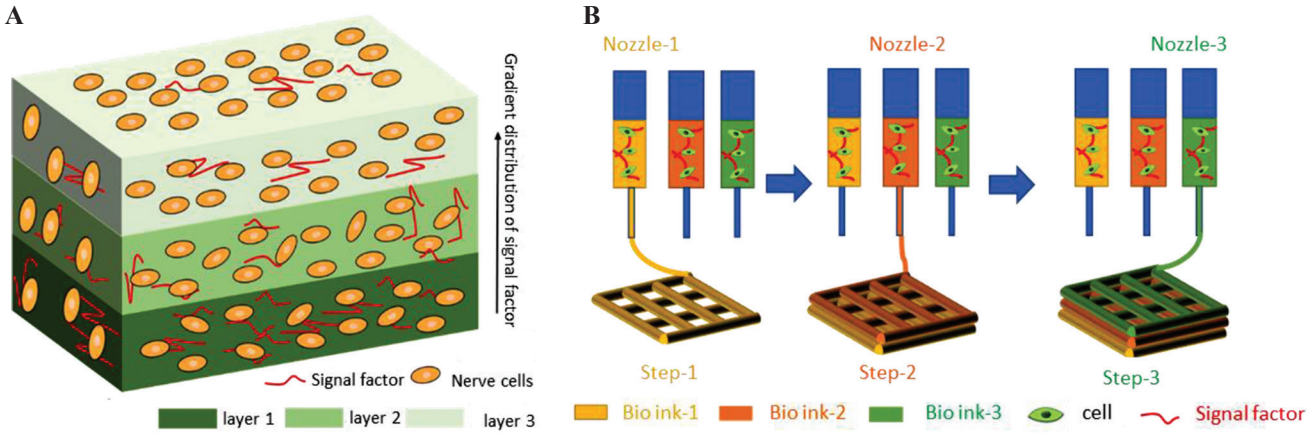

Figure 2. Printing a layered gradient structure that mimics the cortex. (A) Schematic diagram of the layered gradient brain-like model\ designed in the current study. (B) The printing principle of the layered gradient brain-like structure.

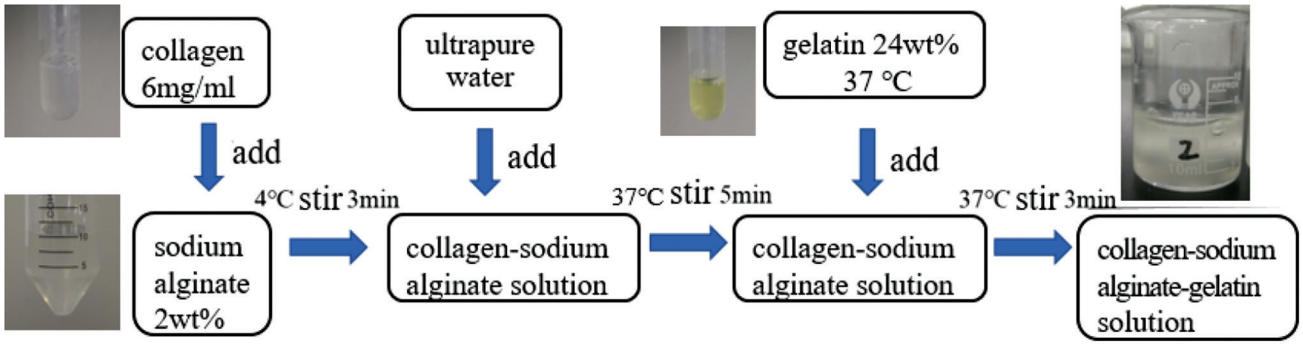

Figure 3. Configuration process of the bio-ink.

The pH value of the bio-inks was adjusted to 7.4 with 0.5M NaOH solution (Tianjin, Tianli), and then the U87 cells were mixed with the bio-inks to obtain the bio-inks with 1×10^6 cells/ml.

2.4. Determination of viscosity

The SNB-1 digital viscometer (Shanghai Nirun, measuring accuracy is ±1.0%) was used to measure the viscosity of the bio-ink. The bio-ink was placed in the metal measuring cylinder of the viscometer. After a series of rotor speed were set, respectively, the viscosity data of the bio-inks under the corresponding speed were recorded.

2.5. Test of compression modulus

The electronic universal testing machine (ETM103A, Shenzhen Wance Testing Equipment Company, China) was used to measure the compression modulus of the bio-ink. The loading speed was set to 1 mm/min, and the compression stroke was set to1.5 mm. Each sample was measured 3 times, and the number of samples is more than or equal to 3, and the variance analysis method was adopted for data analysis.

2.6. Observing the distribution and morphology of pore sizes

Scanning electron microscope (SEM, SU-8010, Japan) was used to analyze the micro-morphology of the internal pores of the printed structure. First, the printed structures were freeze-dried in a freeze-dryer (VFD2000, BIOCOOL, China) for 24 h. After the samples were taken out, the surface of the samples was sprayed with gold; finally, SEM was used to analyze the morphology and pore size of the printed structure.

2.7. Research on the printing parameters

The effects of needle diameter D, material extrusion rate u, and platform moving speed v on the performance of the printed structures were studied by designing orthogonal experiments. Three parameters for each variable were used and the L9 (3^4) orthogonal table (**Table 2**) was selected to design the orthogonal experiment. The printing effect of the printed structures was evaluated by two indexes: Line width and forming accuracy. The forming accuracy, A, of the printed structure was expressed by the following formula:

$$A = \left(1 - \left|\frac{l_1^2 - l^2}{l^2}\right|\right) \times 100\% \qquad (2.1)$$

where l, side length of design; l_1, average side length of the printed structure.

2.8. Determination of cell viability

The LIVE/DEAD®Viability/Cytotoxicity Kit reagent (L3224, Thermo, USA) was used to determine the viability of cells. Using a laser scanning confocal microscope (A1, Nikon, Japan) to observe the fluorescence image of cells, the living cells were labeled with green fluorescence, and the dead cells were labeled with red. Cell viability is expressed as the proportion of the stained green cells in the total number of stained cells. Image J software was used to count the number of the dead/living cells.

Table 2. Factor level table

Factor level	Experimental factors		
	Material extrusion rate μl/min	Platform movement speed mm/s	Needle diameter
	A	B	C
1	30	5	20G
2	60	10	23G
3	120	15	27G

2.9. Statistical analysis

Image J and Microsoft Excel 2010 were used for statistical analysis. Unless otherwise stated, all experiments were conducted independently for at least 3 times. The data were expressed as mean ± standard deviation. Statistical significance within the groups was tested by one-way analysis of variance (ANOVA) and statistical significance between the groups was tested by two-way ANOVA. $P < 0.05$ was considered statistically significant and the $P < 0.01$ was considered very significant.

3. Results

3.1. Influence of pre-treatment time at 4 on the performance of bio-inks

Pre-cooling the G6A1C1 bio-ink in a refrigerator at 4°C was used as the pre-treatment condition of the bio-ink and we studied the effect of the pre-cooling time on the performance of the printing ink. After the bio-inks were placed at 4°C for 0 min, 3 min, 6 min, 9 min, and 12 min, the viscosity of the mixed bio-inks increased rapidly with the increase of the pre-treatment time at low temperature (**Figure 4A**). When the bio-inks were placed at 4°C for 3 min and 6 min, the viscosity of the bio-inks was roughly the same. The viscosity of the bio-inks placed at 4°C for 9 min is about 10 times that of those for 6 min. With the increase of the pre-treatment time (**Figure 4A**), the shape of the extruded ink (**Figure 4B**) changed from spheroidal to linear. When the bio-ink was placed at 4°C for 9 min, the extruded ink was smooth with line shape, and the printed structure (**Figure 4C**) was regular with smooth surface. Therefore, placed the bio-ink at 4°C for 9 min was chosen as the appropriate pre-treatment time in this experiment.

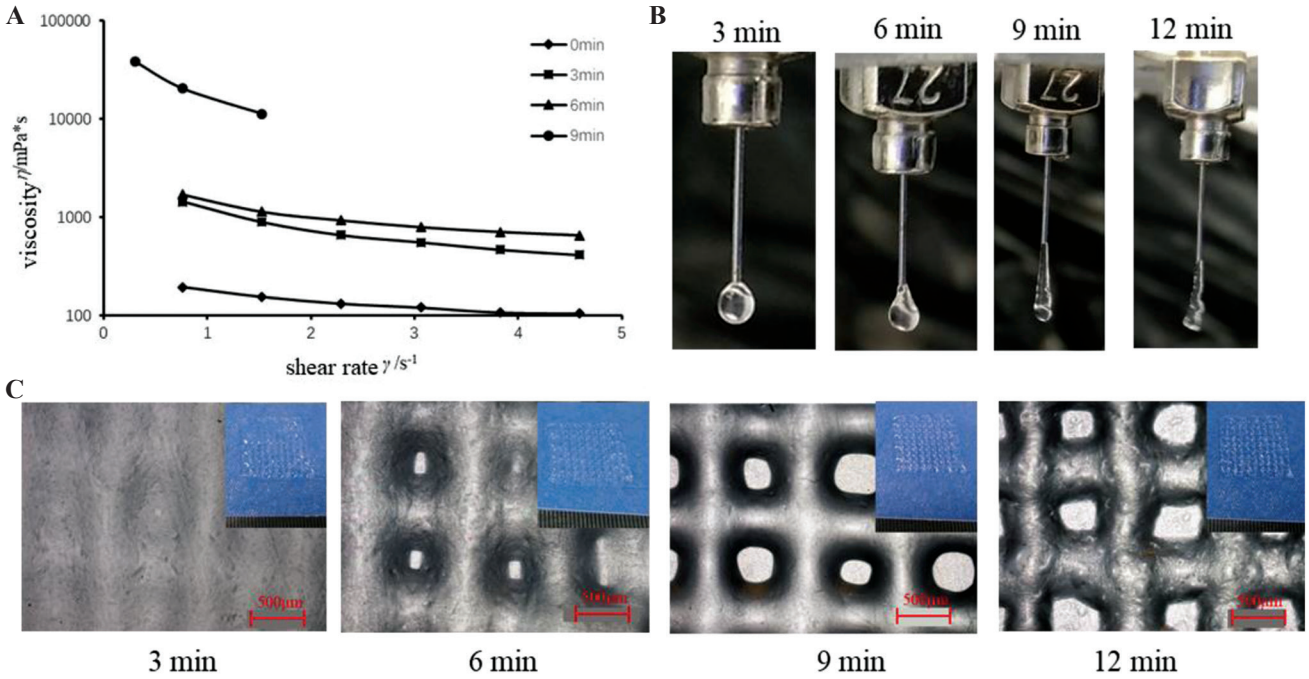

Figure 4. Effect of different pre-cooling time at 4°C on the performance of the G6A1C1 bio-inks. (A) Curve of viscosity and shear rate of the mixed bio-inks. (B) Outflow state of the bio-inks. (C) The micro-morphology of the printed structures printed by the bio-inks with different pre-cooling time.

3.2. Determining the printing parameters of the G6A1C1 bio-ink

The G6A1C1 bio-ink was used to print a single-layer grid structure with side length of 12 mm and spacing of 2 mm. The order of the influence of the printing parameters on the line width (**Table 3**) and forming accuracy (**Table 4**) of the printed structure was as follows: Needle diameter D > moving speed v > extrusion rate u. Needle diameter D ($P < 0.01$) and moving speed v ($P < 0.05$) had significant effects on the line width. These three factors had no significant effect on the forming accuracy.

According to the results of these two evaluation indexes, the optimal printing parameter for the G6A1C1 bio-ink to print the single-layer structure was chosen as follows: The diameter D of the needle was 27G, the moving speed v was 15 mm/s, and the extrusion rate u was 60 μl/min. When using this printing parameter to print a multi-layer structure, it was found that the extruded inks could not deposit continuously due to the fast-moving speed (**Figure 5D**). Therefore, it was necessary to optimize the printing parameters when printing a multi-layer structure. The continuity and stability of the printed multilayer structure can be guaranteed by reducing the moving speed (**Figure 6**). Therefore, according to the experimental results, the printing parameters of multi layer structure were determined as shown in **Table 5**.

Table 3. Range and variance analysis data of line width of the printed structure

Type of data processing	Factor A	Factor B	Factor C
Range analysis			
k1	730.73	856.53	1213.13
k2	761.60	786.60	559.40
k3	811.60	660.80	531.40
Range	80.87	195.73	653.73
Sequence	C>B>A		
Optimal levels	A1	B3	C3
Optimal combination	A1B3C3		
Variance analysis			
Mean-square value	4996.1	29513.9	446455.8
F value	5.397	31.883	482.298
Significance level (P value)	---(0.156)	*(0.030)	**(0.002)

3.3. Effect of post-processing on the performance of the printed structure

(1) Effect of temperature on the performance of the printed structures

G6A1C1 bio-ink was used to print a grid structure with 15 layers. The printed structure was immersed into a solution containing 1% $CaCl_2$ for 30 min at 20°C and 37°C, respectively. The compression modulus of the

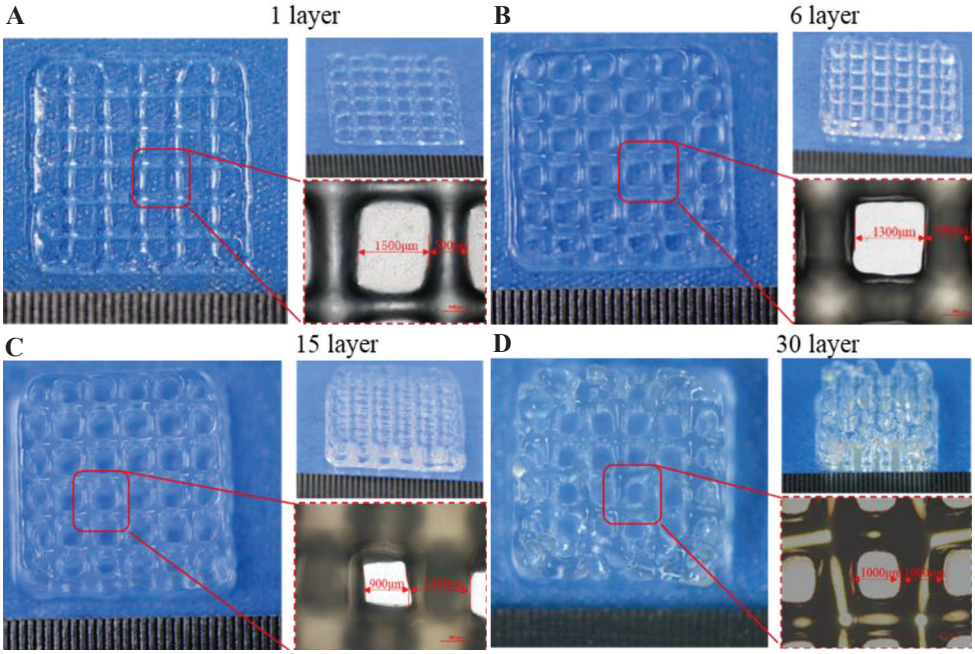

Figure 5. Effect of multi-layer structure printing with optimized single-layer printing parameters.

Table 4. Range and variance analysis data of forming precision

Type of data processing	Factor A	Factor B	Factor C
Range analysis			
k1	91.79	90.45	88.22
k2	95.57	93.34	94.91
k3	91.68	95.24	95.91
Range	3.90	4.79	7.69
Sequence	C>B>A		
Optimal levels	A2	B3	C3
Optimal combination	A2B3C3		
Variance analysis			
Mean-square value	16.06	19.00	56.93
F value	1.25	1.48	4.44
Significance level (*P* value)	---(0.444)	---(0.403)	---(0.184)

printed structure was 5.3 ± 1.3 kpa when treated at 20°C, and 8.1 ± 1.5 kpa while treated at 37°C. After the samples were freeze-dried and scanned by SEM, it was found that there were evenly distributed pores in the printed structure, and the average pore diameters of the pores were 46 ± 10 μm when treated at 20°C, and 44 ± 7 μm when treated at 37°C, and there was no significant difference between the pore sizes when the samples were treated at different temperatures. To meet the low elastic modulus of the cortical tissue, the post-treatment temperature was selected as 20°C in this experiment.

(2) Effect of the concentration of Ca^{2+} on the performance of the printed structure

G6A1C1 bio-ink was used to print a grid structure with 15 layers. In order to verify the effect of the concentration Ca2+ on the performance of the printed structure, we guaranteed that the soaking temperature was 37°C and the soaking time was 30 minutes. With the increase of the concentration of Ca^{2+}, the compression modulus of the printed structure (**Figure 7F**) also increased. The modulus of the printed structure treated with 5% $CaCl_2$ solution (9.57 ± 2.39kpa) was about twice as much as that treated with 0.1% $CaCl_2$ solution (5 ± 2.55 kpa). After freeze-drying, we found that with the increase of the concentration of Ca^{2+} (**Figure 7A-E**), the internal pore size of the printed structure gradually decreased. The internal pore size of the printed structure treated with 0.1% $CaCl_2$ solution (92.3 ± 7.4 μm) was about 5 times as much as that treated with 5% $CaCl_2$ solution. According to the characteristics of the pore size of the cortical tissue, 0.1% $CaCl_2$ solution was used for post-processing in this experiment.

3.4. Physical characterization of the layered structure

Three kinds of nozzles which contains the bio-inks in the order as follows: G6A1C1.5->G6A1C1->G6A1C0.5 were used in turn to print a layered structure. All bio-inks are printed with their optimized printing parameters, and after printing, the printed structure was immersed into a solution containing 0.1% $CaCl_2$ for 30 min at 20°C. It was found that the printed structure was complete and regular,

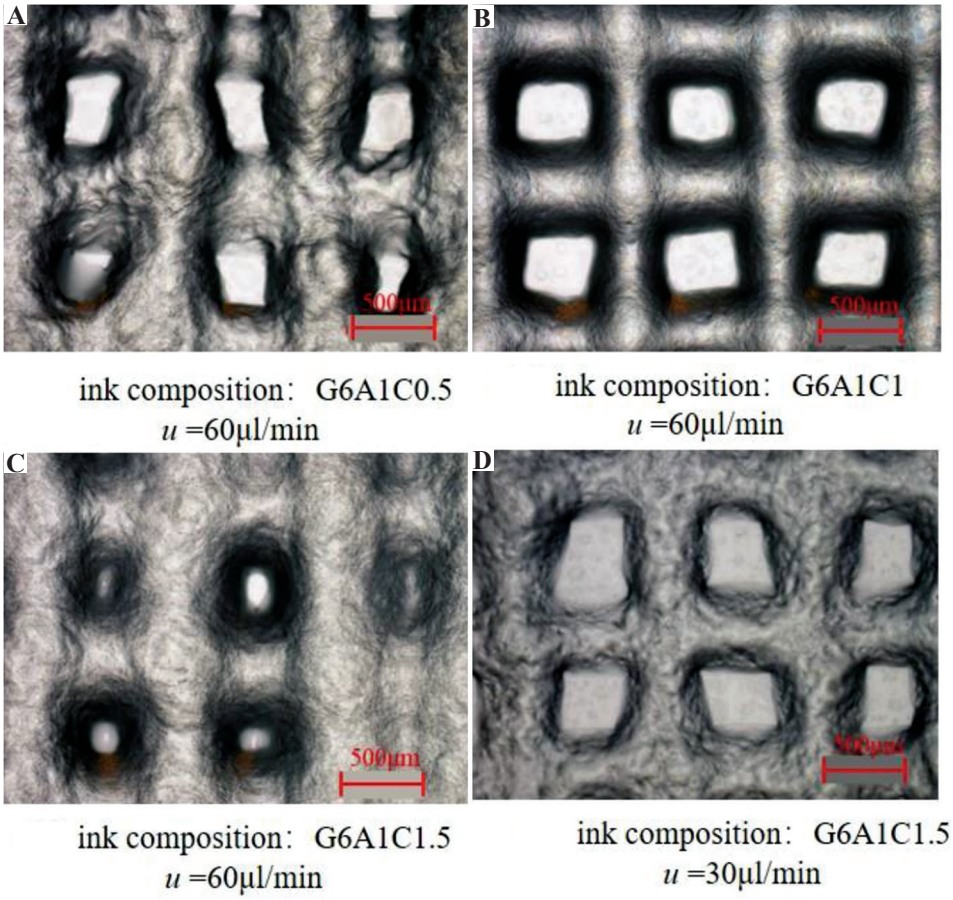

Figure 6. The use of different printing parameters to print the structure with different collagen concentrations in the ink.

which also has obvious layered characteristics and clear grid lines in the middle part (**Figure 8A**). The overall compression modulus (**Figure 8B**) of the total layered structure was 3.7 ± 0.8 kPa (n = 3). The pore size of the layered structure showed a clear gradient distribution (**Figure 8C**). With the decrease of the concentration of the collagen in the bio-inks, the size of the internal pore gradually decreased. The pore sizes of the top part printed with G6A1C1.5 bio-ink were larger than 100 μm when that of the middle part printed with G6A1C1 bio-ink were between 30 and 60 μm, and that of the bottom part printed with G6A1C0.5 bio-ink was the smallest, ranging from 20 μm to 30 μm.

3.5. Biological evaluation of the gradient structure

After the layered tissue was cultured in a cell incubator for 1 day, it was found that the grid structure remained intact (**Figure 9A**). Cells were evenly distributed inside of the printed structure, and most of the cells were living cells with a survival rate of 94.5%. With the increase of the culture days (**Figure 9C-E**), the number of the living cells increased significantly, which indicated that the cells can proliferate rapidly in this printed structure.

4. Discussion

In this study, a set of integrated equipment for cell printing/culturing was designed and built. The maximum printing volume of this system can reach 150 mm × 150 mm × 80 mm. It provided the installation location for multiple nozzles and can be used for printing with single nozzles, multiple nozzles, and coaxial nozzles. This equipment can also meet the requirements of hydrogel formation using various cross-linking forms. Most of the existing bio-printers, such as 3D Discovery and BioFactory manufactured by RegenHU company in Switzerland, and INKREDIBLE from CELLINK company in Sweden, are the open printing systems. During the printing process, the printing device needs to be placed on a clean bench to maintain a sterile environment. The integrated equipment for cell printing/culture designed in this paper can provide a sterile environment during the printing process to ensure that the cells cannot be contaminated. At the same time, the equipment can adjust the temperature and humidity of

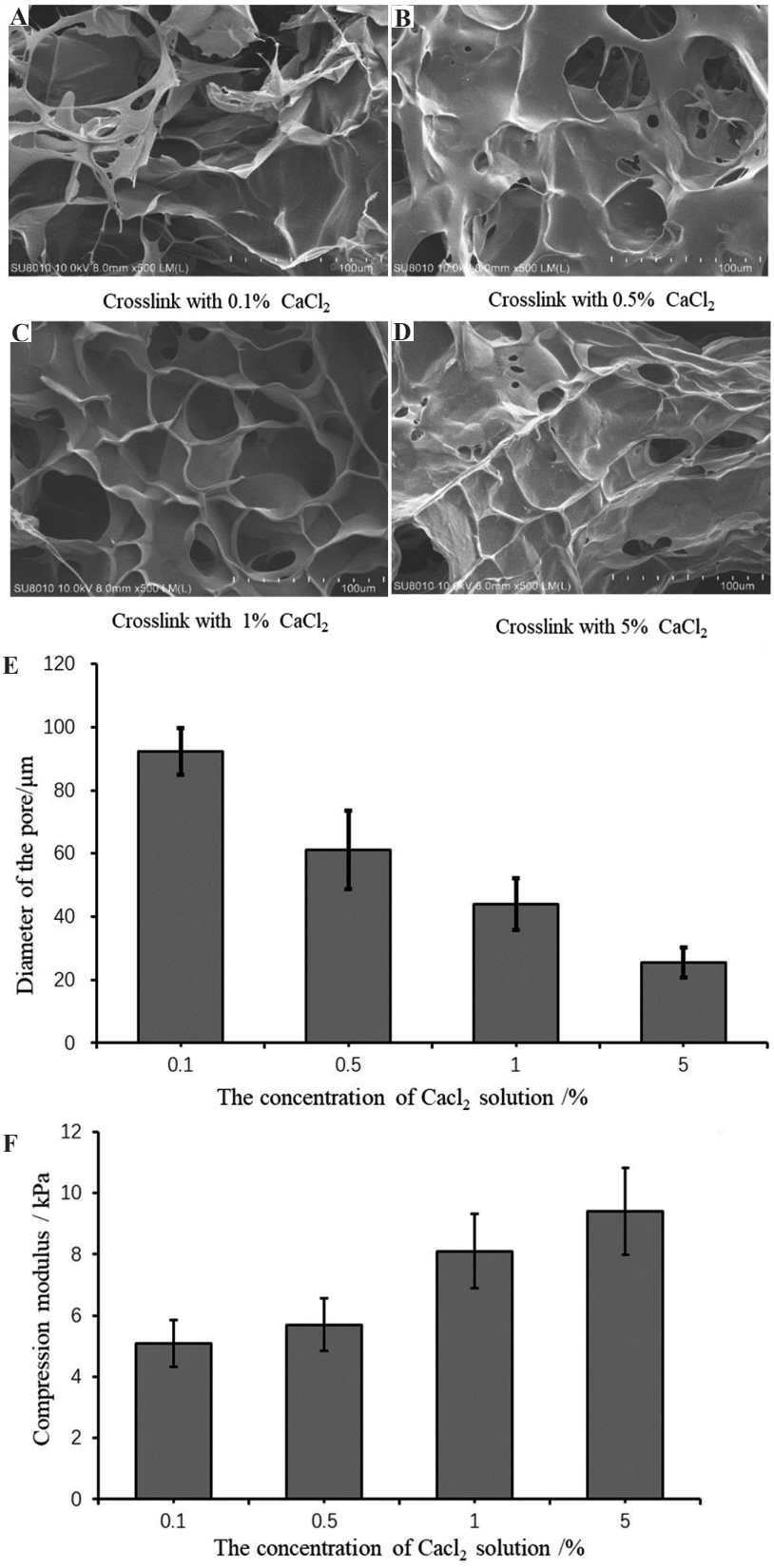

Figure 7. Effect of the concentration of Ca^{2+} on the performance of the printed structure. (A-D) scanning electron microscope image of the morphology of the internal pore of the printed structure. (E) The size of the internal pore of the printed structure. (F) Compression modulus of the printed structure when treated with the different concentration of Ca^{2+} solution.

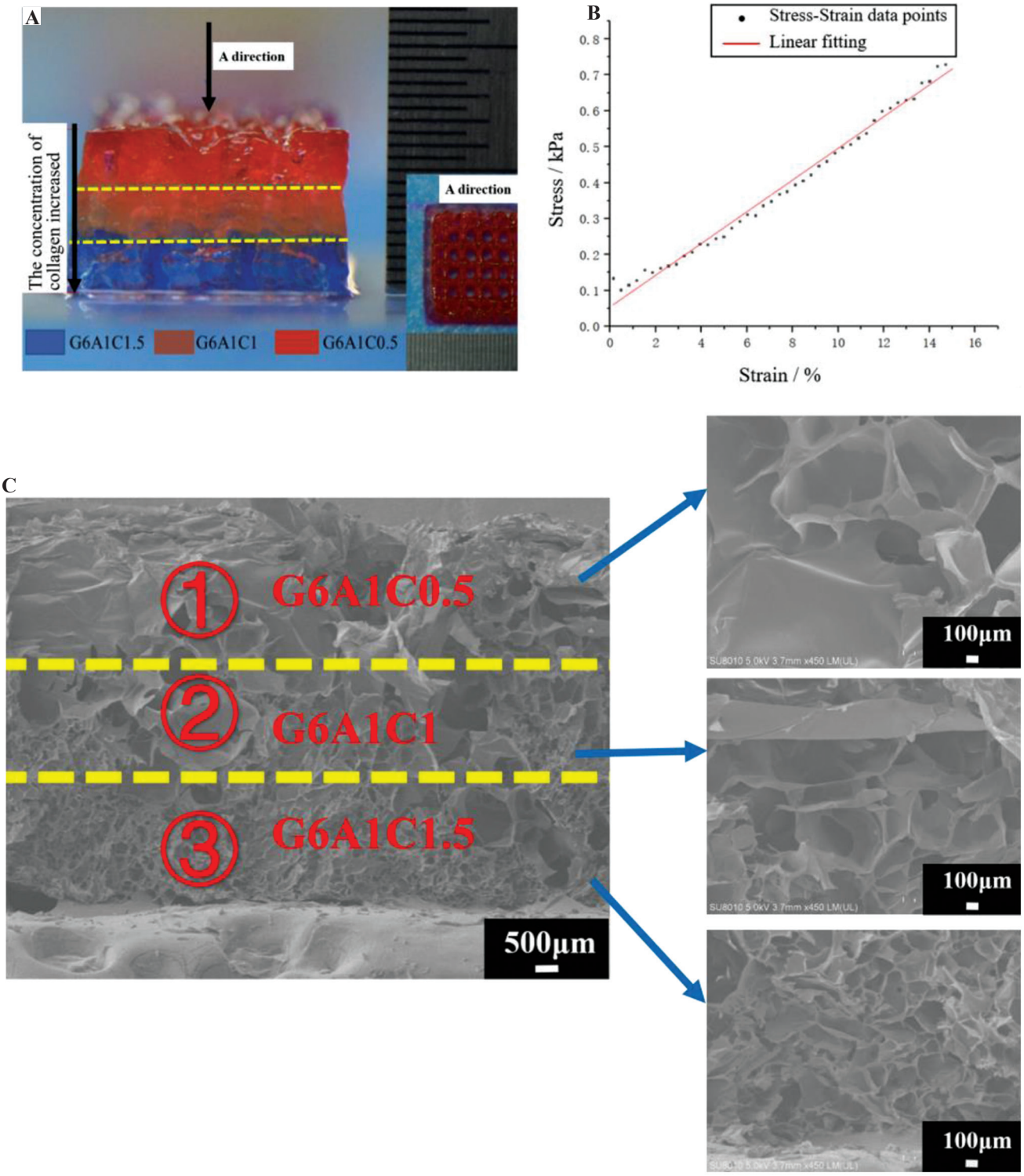

Figure 8. The macro and micro characteristics of the layered structure. (A) The macro-morphology of the layered structure. (B) The stress-strain diagram. (C) The scanning electron microscope image of the cross-section of the layered structure.

the printing room to meet the requirements of cell culture and solve the problem of separation between the printing process and the culture process in the traditional printing method. Meanwhile, the commercial biological 3D printers on the market are expensive, most of which cost between RMB 500,000 and 3 million. In this study, the overall cost of the self-made printing system was about 120,000 RMB, which can substantially reduce the research cost.

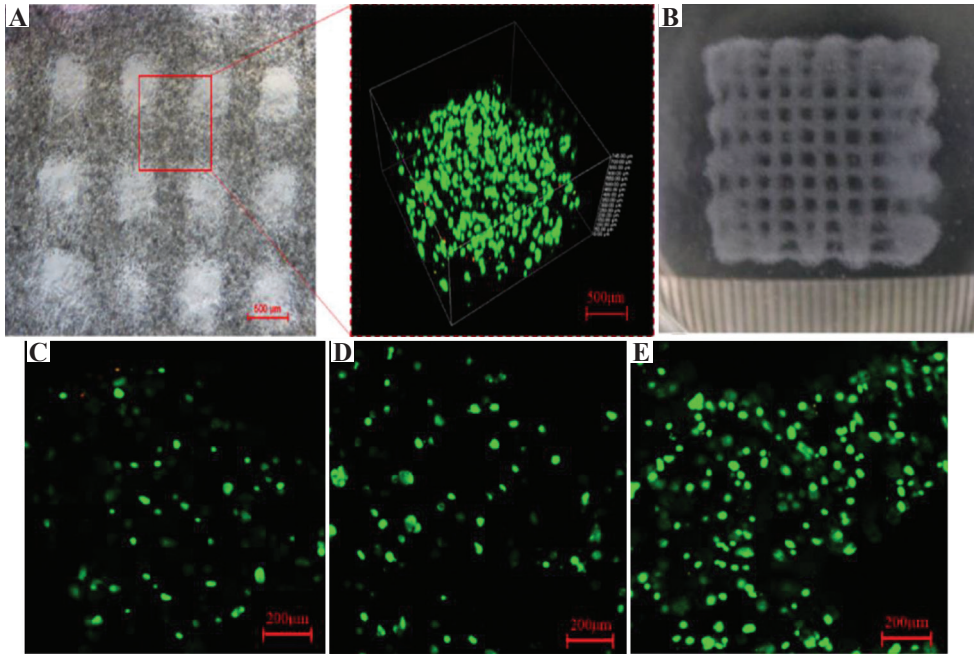

Figure 9. (A) The morphology of the layered structure and the distribution of cells inside of the layered structure which was cultured in a cell incubator for 1 day. (B) The macro morphology of the layered structure when cultured for 7 days. (C-E) The viability of cells in the layered structure when the structure was cultured for 1 day, 3 days, and 7 days, respectively. Green and red fluorescence denote living cells and dead cells, respectively.

Table 5. Printing parameters of bio-inks with different collagen concentration

Parameter type	Ink composition	Needle diameter D (μm)	Extrusion rate of the ink *u* (μl/min)	Moving speed of platform *v* (mm/s)
Top layer	G6A1C0.5	200 (27G)	60	10
Middle layer	G6A1C1	200 (27G)	60	10
Bottom layer	G6A1C1.5	200 (27G)	30	10

Due to the complexity of the brain structure, humans attempt to construct brain-like tissue models *in vitro* to study the structure and function of the brain. At present, Chwalek *et al*.[42] have used the molding method to produce a donut-shaped silk-collagen protein scaffold which can form a 3D neural network that has similar electrophysiological characteristics as normal neural tissue. Odawara *et al*.[43] developed a technique to form the directional fibers using collagen gel and also developed a 3D culture method in a polydimethylsiloxane micro-chamber. Finally, they proved that this method could generate a 3D neural network by accurately controlling the location of the cells. These studies built a 3D neural tissue model *in vitro* using the molding method. Although this method was simple to operate, had low requirements for forming, and did not require complex external conditions, it was difficult to manufacture complex structures, and at the same time, it was impossible to accurately control the density and spatial distribution of the nerve cells. Therefore, it was difficult to produce complex brain-like tissues that bear a high resemblance to the brain. Lee *et al*.[44] proposed a direct ink-jet 3D printing method with multi-layer collagen gel containing rat embryonic astrocytes and neurons. Gu *et al*.[45] proposed a direct printing method using a new bio-ink combining human neural stem cells to print a 3D porous grid structure. These methods can be used to construct 3D brain like tissue by 3D printing, but the brain like tissue constructed by these methods does not simulate the hierarchical structure and gradient characteristics of brain tissue, which verified the feasibility of using the printing method to construct brain-like tissues but lacked the simulation of the layered structure and gradient characteristics of brain tissues. Lozano *et al*.[46] used a peptide-modified gellan gum to prepare a three-layer brain-like layered structure by hand-held extrusion printing method. This study preliminarily simulated the layered structure with or without cells, but it was quite different from the continuous layered structure of natural brain tissue. Gu *et al*.[47] developed a novel and optically visible bio-ink for printing 3D neural tissue. The bio-inks can

maintain good molding accuracy after gelation. Then, the samples were stained to characterize the alive and dead cells, and it was found that there were many dead cells after 1 day of printing. Of note, the survival rate of the cells in the printed structure in our research was maintained at 94.5%. Vijayavenkataraman *et al*.[48] developed a biodegradable conductive hydrogel to provide a conductive environment for the proliferation and differentiation of neurons. However, nerve cells have extremely demanding requirements for the growth environment. The printing system constructed in this study cannot adjust the temperature and humidity in the printing environment during the printing process, thereby providing a sterile environment that is more suitable for the growth of nerve cell. In our research, we constructed a cell printing/culturing integrated operating system that can provide a suitable environment for cell growth during the printing process. Moreover, the overall modulus of the printed tissue constructed in our study is 3.7 ± 0.8 kPa, while the neurons prefer a softer substrate[49].

In view of the low elastic modulus and layered structure of the natural cerebral cortex, this paper proposed a method for manufacturing the layered structure with a gradient distribution of pore size. The density and position of cells in the printed structure can be precisely controlled by extrusion 3D printing technology. By controlling the different nozzles which contain different bio-inks to print the structure in turn, the layered structure can be manufactured. By changing the concentration of collagen in the bio-ink, it is possible to achieve the gradient change of pore size in the printed structure. As the collagen concentration increased from 0.5 mg/ml to 1.5 mg/ml, the pore size of the printed structure also showed a significant increase, thereby realizing the goal of manufacturing a layered structure with gradient pore sizes that mimic the cortex *in vitro*. At the same time, by changing the printing path, more complex tissue models can be printed *in vitro*.

At present, more and more studies have shown that changing the concentration of one or several biomaterials in the mixed bio-inks can change the internal pore size of the printed tissue so as to manufacture the gradient porous structure with heterogeneity. For example, Xu *et al*.[31] obtained smaller internal pore size by increasing the concentration of GelMA in hybrid bio-inks. Ng *et al*.[14] based on the principle of macroporous crowding and adopted the drop-on-demand technology to print the samples, their experimental results have indicated that the layered structures could be achieved by controlling the number of microporous-based bio-ink drops printed on each printed collagen layer. In this study, all parameters remained unchanged, with the exception of the collagen concentration in the mixed bio-ink. Fischer[50] proved that a higher concentration of collagen can lead to a smaller internal pores size of the structure. Therefore, this highlights that the change of pore size as mentioned in this paper is caused by the change of collagen concentration.

Based on the properties of collagen forming at high temperature and that of gelatin forming at low temperature, a set of ink mixing schemes has been developed to minimize the loss of the bio-inks during the mixing process as much as possible. This paper also focuses on the effect of the printing performance of the bio-inks by adjusting the printing parameters. By designing the orthogonal experiment, we found that the diameter of the needle had the most significant influence on the line width of the printed structure, and the moving speed has the second most significant impact. These findings can provide some guidance in the selection and optimization of the printing parameters in the future.

In this study, we have further studied and optimized the printing process. In the preliminary study, we determined that the pre-treatment time of the bio-inks at low temperature was a key parameter that affected the printing performance of bio-inks. When the pre-treatment time was 3 min or 6 min, the extrusion form of the bio-ink was spherical, and the printed grid structure appeared to adhere to each other. These phenomena indicated that the bio-ink tended to be at liquid state, which was mainly related to the characteristics of gelatin forming at low temperature. Thus, if the pre-treatment time was too short, the formation of gelatin would become incomplete, manifested by the collapse and adherence of printed structures. When the processing time was 12 min, the bio-ink had a rough surface morphology, indicating that the gelatin has been basically formed at this time and can be printed. However, at this time, the surface of the printed structure was too rough due to the over-molding. Based on these observations, we determined 9 min as the appropriate pre-treatment time at 4°C.

The main purpose of the post-processing in this study was to reduce the compression modulus of the printed structure and obtain a smaller aperture range (30 – 150 μm). The higher the concentration of Ca^{2+}, the greater the osmotic pressure between the printed tissue and the post-processed solution. The main reason of this phenomenon was that the increased concentration of Ca^{2+} would cause the printed tissue to be more fully cross-linked. Therefore, as the concentration of Ca^{2+} increased, the compressive modulus of the printed structure increased, and the pore size decreased. The total compression modulus of 3D brain-like nerve tissue printed by Gu *et al*.[45] was about 7.5 kPa, while that of the printed structure reported in this paper was about 3.7 kPa. The total compression modulus of the printed structure in our study was reduced by half compared to the results of Gu *et al*.[45], which was closer to that of natural brain tissue.

According to the layered characteristics of the brain tissue, in this paper, we developed a technology to print the layered structure with gradient distribution of pore size. This technology not only be used to manufacture brain-like tissue with layered structure, but also can be used to manufacture layered tissues widely existing in human body, such as cartilage, blood vessels and others. By changing and optimizing the cell type and cell density used in this printing process, we can construct the corresponding tissue/organ *in vitro*.

We encountered some problems in this study. A printed structure of <30 layers can maintain a more regular and complete structure, but when the printed structure had more than 30 layers, the edge of the printed structure began to appear defects, but the middle part could still maintain a better structure. In future research, we plan to further optimize the printing parameters and printing process to produce a structure with more layers. Although the cells possess a high survival rate and proliferation rate within the printed structure, they did not exhibit similar spreading and migration characteristics as in normal tissues. The biocompatibility of the bio-ink can be improved by modifying the material (RGD peptide modification) or adding bioactive factors (structural protein, glycoprotein, etc.) so as to further investigate the effect of special structure or signal factors (gradient distribution) on cell morphology and function expression.

5. Conclusion

In this study, we designed and built integrated cell printing/culture equipment for printing and culturing a 3D brain-like layered structure. This equipment provides a more affordable, integrated, and cell-friendly device for printing active organs and tissues *in vitro*. Gelatin, sodium alginate, and collagen were chosen as the raw materials of printing ink, and we developed a set of preparation scheme of the bio-inks. The optimum printing parameters of the bio-inks were determined by studying the printing process parameters such as material extrusion rate *u*, platform moving rate *v,* and needle diameter D. The pre-treatment and post-processing conditions of the bio-inks were also studied. By adjusting the collagen concentration of the bio-inks in each printing nozzle, the layered structure with gradient distribution of pore size could be produced. The forming accuracy of the printed single-layer structure reached 97.24%, and the survival rate of cells in the printed structure reached 94.5%. These gradient pore structures provide a more accurate 3D *in vitro* model for studying the complex structure and function of brain tissue.

Acknowledgments

The work was supported by the Program of the National Natural Science Foundation of China (51675411), and the Fundamental Research Funds for the Central Universities, and the Youth Innovation Team of Shaanxi Universities.

Conflicts of interest

We have no financial and personal relationships with other people or organizations that can inappropriately influence our work, there is no professional or other personal interest of any nature or kind in any product, service, and/or company that could be construed as influencing the position presented in, or the review of, this article.

Author contributions

J.H. is one of the guest editors of the Special Issue: Bioprinting of 3D Functional Tissue Constructs. The editorial and peer-review processes of this paper was exclusively handled by the editors of the journal without interference of any of the guest editors.

References

1. Muming Pu BX, 2016, Nao Ke Xue Yu Lei Nao Yan Jiu Gai Shu. [Brain Science and Brain-Inspired Intelligence Technology]. *J Chin Acad Sci*, 31:725–36.
2. Xiong Y, Mahmood A, Chopp M, 2013, Animal Models of Traumatic Brain Injury. *Nat Rev Neurosci*, 14:128–42. https://doi.org/10.1038/nrn3407
3. Huh D, Hamilton GA, Ingber DE, 2011, From 3D Cell Culture to Organs-on-Chips. *Trends Cell Biol*, 21:745–54. https://doi.org/10.1016/j.tcb.2011.09.005
4. Imamura Y, Mukohara T, Shimono Y, *et al.*, 2015, Comparison of 2D- and 3D-Culture Models as Drug-testing Platforms in Breast Cancer. *Oncol Rep*, 33:1837–43. https://doi.org/10.3892/or.2015.3767
5. Tian XF, Heng BC, Ge Z, *et al.*, 2008, Comparison of Osteogenesis of Human Embryonic Stem Cells within 2D and 3D Culture systems. *Scand J Clin Lab Invest*, 68:58–6. https://doi.org/10.1080/00365510701466416
6. Zhang D, Pekkanen-Mattila M, Shahsavani M, *et al.*, 2014, A 3D Alzheimer's Disease Culture Model and the Induction of P21-Activated Kinase Mediated Sensing in iPSC Derived Neurons. *Biomaterials*, 35:1420–8. https://doi.org/10.1016/j.biomaterials.2013.11.028
7. Ng WL, Chua CK, Shen YF, 2019, Print Me An Organ! Why We Are Not There Yet. *Prog Polym Sci*, 97:101145. https://doi.org/10.1016/j.progpolymsci.2019.101145
8. Ozbolat IT, Hospodiuk M, 2016, Current Advances and Future Perspectives in Extrusion-based Bioprinting. *Biomaterials*, 76:321–43. https://doi.org/10.1016/j.biomaterials.2015.10.076

9. Zhuang P, Ng WL, An J, *et al.*, 2019, Layer-by-layer Ultraviolet Assisted Extrusion-based (UAE) Bioprinting of Hydrogel Constructs with High Aspect Ratio for Soft Tissue Engineering Applications. *PLoS One*, 14:e0216776. https://doi.org/10.1371/journal.pone.0216776
10. Melchels FP, Feijen J, Grijpma DW, 2010, A Review on Stereolithography and its Applications in Biomedical Engineering. *Biomaterials*, 31:6121–30. https://doi.org/10.1016/j.biomaterials.2010.04.050
11. Saunders RE, Derby B, 2014, Inkjet Printing Biomaterials for Tissue Engineering: Bioprinting. *Int Mater Rev*, 59:430–48. https://doi.org/10.1179/1743280414y.0000000040
12. Koch LG, Unger C, Chichkov B, 2013, Laser Assisted Cell Printing. *Curr Pharm Biotechnol*, 14:91–7.
13. Ng WL, Lee JM, Yeong WY, *et al.*, 2017, Microvalve-based Bioprinting-process, Bio-inks and Applications. *Biomater Sci*, 5:632–47. https://doi.org/10.1039/c6bm00861e
14. Ng WL, Goh MH, Yeong WY, *et al.*, 2018, Applying Macromolecular Crowding to 3D Bioprinting: Fabrication of 3D Hierarchical Porous Collagen-based Hydrogel Constructs. *Biomater Sci*, 6:562–574. https://doi.org/10.1039/c7bm01015j
15. Tobin DJ, 2006, Biochemistry of Human Skin--our Brain on the Outside. *Chem Soc Rev*, 35:52–67. https://doi.org/10.1039/b505793k
16. Ng WL, Wang S, Yeong WY, *et al.*, 2016, Skin Bioprinting: Impending Reality or Fantasy? *Trends Biotechnol*, 34:689–99. https://doi.org/10.1016/j.tibtech.2016.04.006
17. Ng WL, Qi JT, Yeong WY, *et al.*, 2018, Proof-of-concept: 3D Bioprinting of Pigmented Human Skin Constructs. *Biofabrication*, 10:025005. https://doi.org/10.1088/1758-5090/aa9e1e
18. Meek KM, Knupp C, 2015, Corneal Structure and Transparency. *Prog Retin Eye Res*, 49:1–16.
19. Ferreira AM, Gentile P, Chiono V, *et al.*, 2012, Collagen for Bone Tissue Regeneration. *Acta Biomater*, 8:3191–200. https://doi.org/10.1016/j.actbio.2012.06.014
20. Yao HB, Fang HY, Wang XH, *et al.*, 2011, Hierarchical Assembly of Micro-/Nano-building Blocks: Bio-inspired Rigid Structural Functional Materials. *Chem Soc Rev*, 40:3764–85. https://doi.org/10.1039/c0cs00121j
21. Yang XY, Chen LH, Li Y, *et al.*, 2017, Hierarchically Porous Materials: Synthesis Strategies and Structure Design. *Chem Soc Rev*, 46:481–558. https://doi.org/10.1039/c6cs00829a
22. Levingstone TJ, Matsiko A, Dickson GR, *et al.*, 2014, A Biomimetic Multi-layered Collagen-based Scaffold for Osteochondral Repair. *Acta Biomater*, 10:1996–2004. https://doi.org/10.1016/j.actbio.2014.01.005
23. Tu DD, Chung YG, Gil ES, *et al.*, 2013, Bladder Tissue Regeneration Using Acellular Bi-layer Silk Scaffolds in a Large Animal Model of Augmentation Cystoplasty. *Biomaterials*, 34:8681–9. https://doi.org/10.1016/j.biomaterials.2013.08.001
24. Xu R, Luo G, Xia H, *et al.*, 2015, Novel Bilayer Wound Dressing Composed of Silicone Rubber with Particular Micropores Enhanced Wound Re-Epithelialization and Contraction. *Biomaterials*, 40:1–11. https://doi.org/10.1016/j.biomaterials.2014.10.077
25. Chung EJ, Ju HW, Park HJ, *et al.*, 2015, Three-layered Scaffolds for Artificial Esophagus Using Poly (Varepsilon-caprolactone) Nanofibers and Silk Fibroin: An Experimental Study in a Rat Model. *J Biomed Mater Res A*, 103:2057–65. https://doi.org/10.1002/jbm.a.35347
26. Mi HY, Jing X, Yu E, *et al.*, 2015, Fabrication of Triple-layered Vascular Scaffolds by Combining Electrospinning, Braiding, and Thermally Induced Phase Separation. *Mater Lett*, 161:305–8. https://doi.org/10.1063/1.4937310
27. Wang LR, Thissen H, Jane A, *et al.*, 2012, Screening Mesenchymal Stem Cell Attachment and Differentiation on Porous Silicon Gradients. *Adv Funct Mater*, 22:3414–23. https://doi.org/10.1002/adfm.201200447
28. Wu C H, Lee F K, Kumar SS, *et al.*, 2012, The Isolation and Differentiation of Human Adipose-derived Stem Cells Using Membrane Filtration. *Biomaterials*, 33:8228–39. https://doi.org/10.1016/j.biomaterials.2012.08.027
29. Nam H, Jeong HJ, Jo Y, *et al.*, 2020, Multi-layered Free-form 3D Cell-printed Tubular Construct with Decellularized Inner and Outer Esophageal Tissue-derived Bioinks. *Sci Rep*, 10:7255. https://doi.org/10.1038/s41598-020-64049-6
30. Sun Y, You Y, Jiang W, *et al.*, 2020, 3D Bioprinting Dual-factor Releasing and Gradient-structured Constructs Ready to Implant for Anisotropic Cartilage Regeneration. *Sci Adv*, 6:eaay1422. https://doi.org/10.1126/sciadv.aay1422
31. Xu L, Varkey M, Jorgensen A, *et al.*, 2020, Bioprinting Small Diameter Blood Vessel Constructs with an Endothelial and Smooth Muscle Cell Bilayer in a Single Step. *Biofabrication*, 12:045012.

https://doi.org/10.1088/1758-5090/aba2b6

32. Kato-Negishi M, Morimoto Y, Onoe H, *et al.*, 2013, Millimeter-sized Neural Building Blocks for 3D Heterogeneous Neural Network Assembly. *Adv Healthc Mater*, 2:1564–70. https://doi.org/10.1002/adhm.201300052
33. Sundararaghavan HG, Monteiro GA, Firestein BL, *et al.*, 2009, Neurite Growth in 3D Collagen Gels with Gradients of Mechanical Properties. *Biotechnol Bioeng*, 102:632–43. https://doi.org/10.1002/bit.22074
34. NjNbRU, 2008, Microfluidic Generation of Biomaterial Gradients for Control of Neurite Outgrowth. Graduate School New Brunswick Electronic Theses and Dissertations.
35. Hopkins AM, DeSimone E, Chwalek K, *et al.*, 2015, 3D *In Vitro* Modeling of the Central Nervous System. *Prog Neurobiol*, 125:1–25.
36. Bai H, Wang D, Delattre B, *et al.*, 2015, Biomimetic Gradient Scaffold from Ice-templating for Self-seeding of Cells with Capillary Effect. *Acta Biomater*, 20:113–119. https://doi.org/10.1016/j.actbio.2015.04.007
37. Rnjak-Kovacina J, Wise SG, Li Z, *et al.*, 2011, Tailoring the Porosity and Pore Size of Electrospun Synthetic Human Elastin Scaffolds for Dermal Tissue Engineering. *Biomaterials*, 32:6729–36. https://doi.org/10.1016/j.biomaterials.2011.05.065
38. Murphy CM, Haugh MG, O'Brien FJ, 2010, The Effect of Mean Pore Size on Cell Attachment, Proliferation and Migration in Collagen-glycosaminoglycan Scaffolds for Bone Tissue Engineering. *Biomaterials*, 31:461–6. https://doi.org/10.1016/j.biomaterials.2009.09.063
39. Lu H, Kawazoe N, Kitajima T, *et al.*, 2012, Spatial Immobilization of Bone Morphogenetic Protein-4 in a Collagen-PLGA Hybrid Scaffold for Enhanced Osteoinductivity. *Biomaterials*, 33:6140–6. https://doi.org/10.1016/j.biomaterials.2012.05.038
40. Engelmayr GC Jr., Cheng M, Bettinger CJ, *et al.*, 2008, Accordion-like Honeycombs for Tissue Engineering of Cardiac Anisotropy. *Nat Mater*, 7:1003–10. https://doi.org/10.1038/nmat2316
41. Pham QP, Shrma U, Mikos AG, 2006, Electrospun Poly(E-caprolactone) Microfiber and Multilayer Nanofiber/Microfiber Scaffolds: Characterization of Scaffolds and Measurement of Cellular Infiltration. *Biomacromolecules*, 7:2796–2805. https://doi.org/10.1021/bm060680j
42. Chwalek K, Tang-Schomer MD, Omenetto FG, *et al.*, 2015, *In Vitro* Bioengineered Model of Cortical Brain Tissue. *Nat Protoc*, 10:1362–73. https://doi.org/10.1038/nprot.2015.091
43. Odawara A, Gotoh M, Suzuki I, 2013, A Three-dimensional Neuronal Culture Technique that Controls the Direction of Neurite Elongation and the Position of Soma to Mimic the Layered Structure of the Brain. *RSC Adv*, 3:23620. https://doi.org/10.1039/c3ra44757j
44. Lee W, Pinckney J, Lee V, *et al.*, 2009, Three-dimensional Bioprinting of Rat Embryonic Neural Cells. *Neuroreport*, 20:798–803. https://doi.org/10.1097/wnr.0b013e32832b8be4
45. Gu Q, Tomaskovic-Crook E, Lozano R, *et al.*, 2016, Functional 3D Neural Mini-Tissues from Printed Gel-Based Bioink and Human Neural Stem Cells. *Adv Healthc Mater*, 5:1429–38. https://doi.org/10.1002/adhm.201670060
46. Lozano R, Stevens L, Thompson BC, *et al.*, 2015, 3D Printing of Layered Brain-like Structures Using Peptide Modified Gellan Gum Substrates. *Biomaterials*, 67:264–73. https://doi.org/10.1016/j.biomaterials.2015.07.022
47. Gu ET, Wallace GG, Crook JM, 2017, Engineering Human Neural Tissue by 3D Bioprinting. In: Biomaterials for Tissue Engineering. Methods in Molecular Biology. p129–38. https://doi.org/10.1007/978-1-4939-7741-3_10
48. Vijayavenkataraman S, Vialli N, Fuh JY, *et al.*, 2019, Conductive Collagen/Polypyrrole-b-polycaprolactone Hydrogel for Bioprinting of Neural Tissue Constructs. *Int J Bioprint*, 5:229. https://doi.org/10.18063/ijb.v5i2.1.229
49. Engler AJ, Sen S, Sweeney HL, *et al.*, 2006, Matrix Elasticity Directs Stem Cell Lineage Specification. *Cell*, 126:677–89. https://doi.org/10.1016/j.cell.2006.06.044
50. Fischer T, Hayn A, Mierke CT, 2019, Fast and Reliable Advanced Two-step Pore-size Analysis of Biomimetic 3D Extracellular Matrix Scaffolds. *Sci Rep*, 9:8352. https://doi.org/10.1038/s41598-019-44764-5